Rapid and Visual Detection of *Listeria monocytogenes* Based on Nanoparticle Cluster Catalyzed Signal Amplification

Lisha Zhang, Ru Huang, Weipeng Liu, Hongxing Liu, Xiaoming Zhou, Da Xing

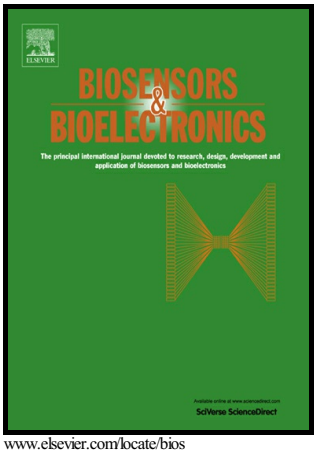

www.elsevier.com/locate/bios

PII: S0956-5663(16)30529-2
DOI: http://dx.doi.org/10.1016/j.bios.2016.05.100
Reference: BIOS8790

To appear in: *Biosensors and Bioelectronic*

Received date: 3 April 2016
Revised date: 30 May 2016
Accepted date: 31 May 2016

Cite this article as: Lisha Zhang, Ru Huang, Weipeng Liu, Hongxing Liu Xiaoming Zhou and Da Xing, Rapid and Visual Detection of *Listeri monocytogenes* Based on Nanoparticle Cluster Catalyzed Signal Amplification *Biosensors and Bioelectronic,* http://dx.doi.org/10.1016/j.bios.2016.05.100

Rapid and Visual Detection of *Listeria monocytogenes* Based on Nanoparticle Cluster Catalyzed Signal Amplification

Lisha Zhang, Ru Huang, Weipeng Liu, Hongxing Liu, Xiaoming Zhou*, Da Xing*

MOE Key Laboratory of Laser Life Science & Institute of Laser Life Science, College of Biophotonics, South China Normal University, Guangzhou, China, CN 510631

xingda@scnu.edu.cn

zhouxm@scnu.edu.cn

*Corresponding authors. Tel: +86-20-85210089; Fax: +86-20-85216052.

Abstract

Foodborne pathogens pose a significant threat to human health worldwide. The identification of foodborne pathogens needs to be rapid, accurate and convenient. Here, we constructed a nanoparticle cluster (NPC) catalyzed signal amplification biosensor for foodborne pathogens visual detection. In this work, vancomycin (Van), a glycopeptide antibiotic for Gram-positive bacteria, was used as the first molecular recognition agent to capture *Listeria monocytogenes* (*L. monocytogenes*). Fe_3O_4 NPC modified aptamer, was used as the signal amplification nanoprobe, specifically recognize to the cell wall of *L. monocytogenes*. As vancomycin and aptamer recognize *L. monocytogenes* at different sites, the sandwich recognition showed satisfied specificity. Compared to individual Fe_3O_4 nanoparticle (NP), NPC exhibit collective effect-enhanced catalytic activity for the color reaction of chromogenic substrate. The change in absorbance or color could represent the concentration of target. Using the Fe_3O_4 NPC-based signal amplification method, *L. monocytogenes* whole cells could be directly assayed within a linear range of 5.4×10^3 - 10^8 cfu/mL and a visual limit of detection of 5.4×10^3 cfu/mL. Fe_3O_4 NPC-based method was more sensitive than the Fe_3O_4 NP-based method. All these attractive characteristics of highly sensitivity, visual and labor-saving, make the biosensor possess a potential application for foodborne pathogenic bacteria detection.

Keywords

Foodborne pathogens; *Listeria monocytogenes*; Vancomycin; Nanoparticle cluster; Poly-L-lysine; Nanoprobe

1. Introduction

Foodborne bacterial have become the major threat of public health worldwide, due to the high incidence of foodborne diseases (Law et al., 2014). The common foodborne pathogens are *Listeria monocytogenes* (*L. monocytogenes*), *Escherichia coli O157: H7* (*E. coil*), *Staphylococcus aureus* (*S. aurens*), *Salmonella enterica* (*Salmenella*) and so on, they are the most common causes of hospitalizations and deaths (Jiang et al., 2016; Lee et al., 2015; Vaisocherová-Lísalová et al., 2016). The conventional identification methods of foodborne pathogens are based on culture and colony counting, which combined with standard biochemical identifications (Shan et al., 2015). Although these methods are usually inexpensive and simple, it is not fit for rapid screen and point-of-care test (POCT) foodborne pathogens, because it demands highly trained personnel, labor-intensive manipulation and several days of culture (Lazcka et al., 2007). Nucleic acid amplification-based methods are widely used for detecting foodborne pathogen, due to the high sensitivity (Chua et al., 2011). The common nucleic acid amplification-based methods have polymerase chain reaction (PCR) (Edwards et al., 1991; McGregor et al., 2010; Zhang et al., 2015), nucleic acid sequence-based amplification (NASBA) (Asiello and Baeumner, 2011; Compton, 1991; Leone et al., 1998), loop-mediated isothermal amplification (LAMP) (Notomi et al., 2000; Parida et al., 2008; Tomita et al., 2008; Van Ness et al., 2003) and so on. However these methods require cell disruption and nucleic acid extracting, they need technical expertise and specialized instruments, thus the nucleic acid-based methods are inappropriate in POCT.

Immunological assay have been widely used for the detection of foodborne pathogens (Valderrama et al., 2015), such as enzyme-linked immunosorbent assay (ELISA). Sandwich ELISA is a common form, which involves two antibodies bind to bacterial at two distinct sites (Zhu et al., 2016).

Nowadays, antibiotics have been used to replace antibody as the recognition agent on microplate (Kong et al., 2015). Since the five-point hydrogen bond binding between the vancomycin (Van) and the D-alanyl-D-alanine (D-Ala-D-Ala) moieties on the cell surface of bacteria (Kell et al., 2008), Van can firmly anchor to most kind of Gram-positive bacteria. The properties of antibiotics such as low cost, good quality controllability and high stability, make it could be an ideal candidate of molecular recognition agents for pathogens detection (Gao et al., 2015; Zhu et al., 2015). After the sandwich molecule recognition structure formed, using the enzyme catalyze substrate to produce colored products, pathogens can be detected by naked-eye. There are different kinds of catalyzing enzymes can be used in sandwich ELISA, such as beta-galactosidase, alkaline phosphatase and horseradish peroxidase (Yang et al., 2016). Currently, natural catalyzing enzyme could be replace by nanoparticle, such as Fe_3O_4 nanoparticle (NP) , which is based on previously findings that Fe_3O_4 NP possess intrinsic peroxidase-like activity, which is similar to the natural peroxidase enzymes (Gao et al., 2007). This type of catalytic inorganic nanomaterial has been termed a nanozyme (Wei and Wang, 2013). Because of their low cost, stability and the ability to be reused, nanozyme have been widely used for biomedical detection and environmental analysis (Fan et al., 2012; Liang et al., 2013; Zhuang et al., 2012). However, currently developed colorimetric immunoassays usually limited by their low sensitivity, due to the low-abundant of detect biomarkers (Gao et al., 2014). It has become a bottleneck for foodborne disease identification. To improve the sensitivity of ELISA, some strategies such as using biotin-streptavidin systems (Qu et al., 2014), enzyme-loaded particles or enzyme-loaded spherical poly (acrylic acid) brushes as labels in ELISA were proposed (De Vocht et al., 2010; Knopp et al., 2009; Tekin and Gijs, 2013).

Here, a nanoprobe-based biosensor, which based on the catalytic properties of the Fe_3O_4 NP and the affinity of vancomycin to the cell wall of *L. monocytogenes*, was constructed. To show the feasibility of the nanoprobe-based biosensor, a proof-of-concept method for *L. monocytogenes* assay was designed. *L. monocytogenes* is a widely distributed Gram-positive bacterium (Azmi et al., 2015), which involved in a variety of dangerous diseases, including septicemia, meningitis, spontaneous abortion and a high fatality rate (30%) (Doumith et al., 2004; Lee et al., 2013). Furthermore, to

improve the sensitivity of the nanoprobe-based biosensor, Fe_3O_4 nanoparticle cluster (NPC) modified aptamer was used as the signal amplification nanoprobe. The Fe_3O_4 NPC was prepared by individual Fe_3O_4 NP cross-linking with poly-L-lysine, compared to individual NP, NPC could exhibit higher catalytic activity, due to the collective effect of NPC. As the NPC-aptamer specially recognized the internalin A protein, Fe_3O_4 NPC catalyzed the substrate to produce colored products, which make the detection of *L. monocytogenes* visualized, without the need for any special equipment. This study illustrates that using the collective effect of Fe_3O_4 NPC could become an effective measure for increasing the sensitivity of the colorimetric assay.

2. Experimental section

2.1. Materials and Reagents

$FeCl_3 \cdot 6H_2O$, ethylene glycol, 1-(3-dimethylaminopropyl)-3-ethylcarbodiimide hydrochloride (EDC), 2-(N-morpholino) ethanesulfonic acid (MES), vancomycin hydrochloride, rhodamine B (RhB), N-hydroxysuccinimide (NHS), poly-L-lysine (PLL, Mw30-70 kDa) were purchased from Sigma-Aldrich (USA). Sodium acetate (NaAc), ethanol and sodium chloride (NaCl) were purchased from the Guangzhou Chemical Reagent Factory (Guangzhou, China). Polyoxyethylene sorbitan monolaurate (Tween-20), Tris buffer (pH 7.4), phosphate buffered saline (PBS), dimethyl sulfoxide (DMSO), bovine serum albumin (BSA), yeast extract, tryptone, and DNA aptamer probes were all purchased from Sangon Biotech Co. Ltd (Shanghai China). The aptamer sequence is 5'NH_2-TTT TTT TTT TAT CCA TGG GGC GGA GAT GAG GGG GAG GAG GGC GGG TAC CCG GTT GAT-3'. 1-Step Ultra-TMB was obtained from Thermo Scientific (Fairlawn, NJ, USA). High-affinity 96-well polystyrene microplates were provided by Corning Costar Co., Ltd. (Germany). Fluorescein isothiocyanate (FITC) was provided by Beyotime Biotechnology Co. Ltd (Shanghai China). All the reagents were analytical grade and used without further purification. Deionized water used throughout the experiments was generated by a Milli-Q water purification system (Millipore, Bedford, MA), and the deionized water had an electric resistance >18.2 MΩ. *Salmonella enterica* (CMCC 50040), *Escherichia coli* (O157:H7 GW1.0202), *Vibrio Parahemolyticus* (ATCC 17802), *Listeria*

monocytogenes (CMCC 54007), and *Staphylococcus aureus* (CMCC 26003) were purchased from Guangzhou Institute of Microbiology (Guangzhou, China). Milk was purchased from the local supermarket. Coating buffer was 0.10 M Tris-HCl buffer (pH 8.5). Blocking buffer was PBS containing 3.0% BSA and 0.05% Tween-20. Washing buffer was PBS containing 0.05% Tween-20. All buffers were sterilized at 121°C for 20 min in an autoclave sterilizer.

2.2. Synthesis and Characterization of Fe_3O_4 NP and Fe_3O_4 NPC

Fe_3O_4 NP was synthesized according to the solvothermal method (Duan et al., 2015). Briefly, a solution of base (20 mL) ethylene glycol was mixed with $FeCl_3 \cdot 6H_2O$ (0.6 g) to form a clear solution, followed by the addition of sodium acetate (1.5 g). The mixture was stirred for 30 min and sealed into a teflon-lined stainless-steel autoclave, and reaction at 200°C for 16 h. Then the autoclave was cooled down to room temperature. The products were washed several times with ethanol and ultrapure water, using a magnetic separator remove the extra solution, then dried the products in vacuum for 12 h. Morphology and structure of Fe_3O_4 NP were characterized with a JEM-2100HR transmission electron microscope (JEOL, Tokyo, Japan).

The Fe_3O_4 NPC was synthesized according to the previous literature (Liu et al., 2011). Briefly, 1 mg EDC was dissolved in PBS by vortexing, 1 mg NP were introduced to the mixture and incubated 30 min at room temperature. Then different amounts of PLL were introduced. After they vortexed and incubated at 4 °C overnight, using a magnetic separator remove the unreacted extra PLL and EDC, then the cross-linking Fe_3O_4 NPC were obtained. Dispersing the NPC in 1 mL PBS solution and stored at 4 °C before next step use.

The hydrodynamic size and zeta potentials of NP and NPC were measured at room temperature in neutral water solution with a Zetasizer Nano ZS (Malvern). (Data are mean ± standard deviation. N = 3 for all groups.)

2.3. Preparation of Nanoprobe

One milligram (mg) Fe_3O_4 NP or NPC were activated by incubation with 1 mg/mL EDC and NHS at room temperature for 30 min, then washed the products twice with PBS. Functionalized NP or NPC incubated with the specific aptamer probe in NaAc buffer (50 mM, pH 6.0). The reactions were

allowed to proceed overnight. Then washed the conjugation twice with PBS, and resuspended in Tris buffer (50 mM, pH 7.2). The mixture incubated at room temperature for 30 min. The nanoprobe were separated and dispersed in 1 mL of PBS, and stored at 4 ℃ for the future detection.

2.4. Conjugation of the BSA-Van

Van were conjugated with BSA by (EDC/sulfo-NHS)-mediated amidation reaction. In a typical protocol, 10 mg of Van was activated by incubation with 300 μL of EDC solution at 20 mg/mL and 300 μL of NHS solution at 1.0 mg/mL. Then 250 μL of protein solution at 1.0 mg/mL was introduced to the activated Van, and vortexed and incubated at 4℃ overnight. 40 μL of Tris-buffer solution (50 mM, pH 7.2) was added to stop the reaction. Removing the unreacted Van and EDC by ultrafiltration using a 10 kDa filter at 5,000 rpm and the detection wavelength is 280 nm. The antibiotic activity of the BSA-conjugated Van (BSA-Van) was investigated by a standard bactericidal halo test.

2.5. Preparing the Nanoprobe-based Biosensior

BSA-Van were added in coating buffer, the 96-well microplate was coated with BSA-Van at 25 μg/mL (100 μL/well) and agitated on a plate shaker (600-700 rpm.) overnight at 4 ℃. Modified wells were then washed thrice with washing buffer (300 μL/well). Then the blocking buffer (150 μL/well) was added into the well and blocking the microplate for 60 min at room temperature. After three times washing, a final addition of 250 μL PBS was used to store the wells until used in experiment.

2.6. Bacteria Sample Preparation

Bacteria strains were grown in lysogeny broth medium at 37 ℃ overnight till optical density value at 600 nm (OD 600) reached 1.0. Optical density value of bacteria solution was detected by an UV-2700 spectrophotometer (Shimadzu Co., Ltd., Japan). The broth mixed 1.0 g of tryptone, 0.5 g of yeast extract, and 1.0 g of NaCl in 100 mL of water. The pH was adjusted to 7.0. Bacteria were harvested at the exponential growth phase by a centrifugation at 5,000 rpm for 5 min and isolated from the broth. The collected pellets were washed twice and resuspended in PBS. Cell numbers of bacteria were determined using a conventional plate counting method, and the results were converted to OD 600 values. All the glassware was sterilized in an autoclave.

2.7. Confocal Microscopy Imaging of Fluorescence-stained *L. monocytogenes*

We added 50 μL of RhB-labeled Van (100 μg/mL) and FITC-labeled aptamer to 100 μL of bacteria solution, followed by an incubation of 1 h in the dark, the concentration of bacteria was 5.4×10^6 cfu/mL. The stained bacteria cells were centrifugally washed thrice and resuspended in MES-buffered water (pH 6). Dropped 12 μL of stained bacteria solution onto a microscope slide, and covered by a cover slip. Then observed the specimen, and the fluorescence micrographs were obtained with a LSM710 laser confocal fluorescence microscopy (Carl Zeiss Co., Ltd., Germany). The excitation wavelengths for RhB and FITC were 543 nm and 488 nm, respectively, while the emission wavelengths for R-PE and FITC were 625 nm and 525nm, respectively。

2.8. Procedure for *L. monocytogenes* Detection

150 μL of sample solution was injected into the well and incubated at room temperature for 30 min. After three times washing, 100 μL of nanoprobe was introduced into the well and incubated for 30 min on a shaker. Removing the unbound probe and wash thrice, 100 μL 1-Step Ultra TMB solution was added into the well, and measuring the absorbance at 652 nm. Also the result of detection can be estimated by naked-eye, though the color intensity.

2.9. Detection of Real Samples

Three sterile milk samples were spiked with different known amounts of *L. monocytogenes*. Additionally, 100 μL of 1×PBS buffer instead of the bacterial strain was used as negative control. The whole samples were analyzed by the nanoparticle cluster catalyzed signal amplification biosensor.

3. Results and Discussion

3.1. Strategy of Nanoprobe-based Biosensor

The principle of nanoprobe-based biosensor is described in Fig. 1. Van was conjugated with BSA, which ensure the Van connected to the microplate through the physical absorption. As a Gram-positive pathogen, *L. monocytogenes* was captured by the Van through the firm five-point hydrogen bond binding between Van and D-Ala-D-Ala moieties in the cell wall, the D-Ala-D-Ala is from N-acetyl-glucosamine peptide and the N-acetylmuramic acid subunits on the cell wall of bacteria.

Apatmer-labeled NP recognized *L. monocytogenes* through the strong and specific binding with the internalin A protein on the surface of the cell (Ding et al., 2014). Thus, the sandwich complex was formed on the microplate, as shown in Fig. 1B. Owing to the intrinsic peroxidase-like activity of Fe_3O_4 NP, the NP probe can generate a color reaction by catalyzing the chromogenic substrate, thereby allowed a direct visual assay of whole cells of *L. monocytogenes*. Furthermore, to improve the sensitivity of the nanoprobe-based biosensor, Fe_3O_4 NPC probe was designed (Fig. 1A). The Fe_3O_4 NPC was synthesized by cross-linking the individual mother Fe_3O_4 nanoparticle with poly-L-lysine, which possesses an amine group in each repeat unit (Lemaitre et al., 1987).This NPC probe has three functions: recognition, visualizing and signal amplification. Using the collective effect of Fe_3O_4 NPC could improve the catalytic ability of the signal probe. That could be an effective signal amplification strategy for the nanoparticle catalyzed colorimetric assay.

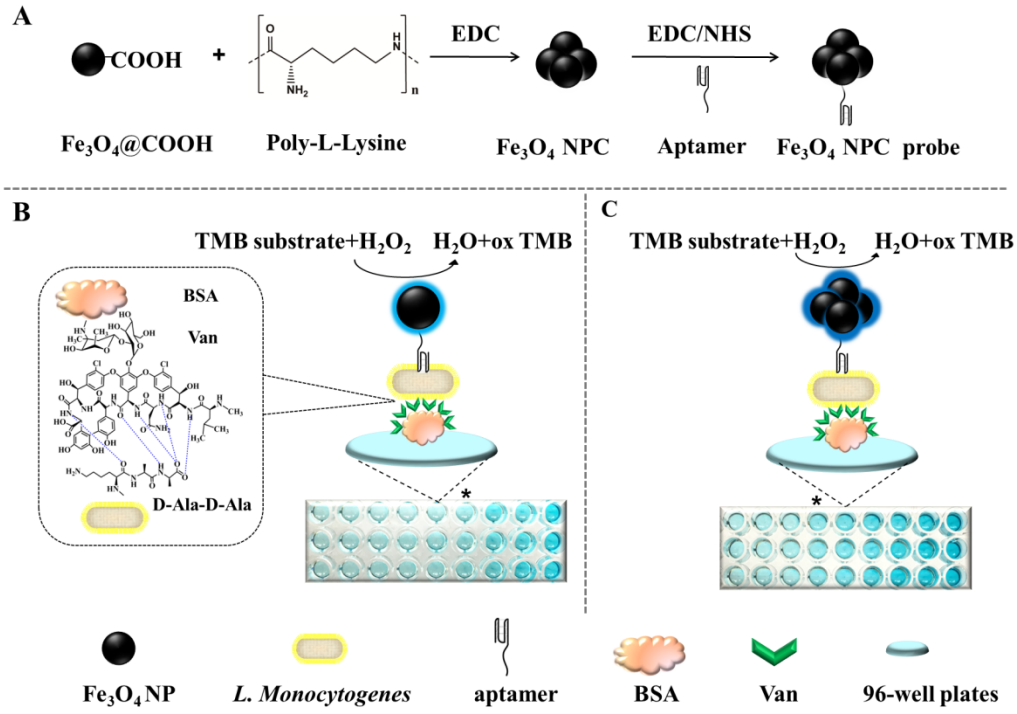

Fig. 1. Schematic representation for the preparation of Fe_3O_4 NPC (A), the principle of the Fe_3O_4 NP -based biosensor (B), and the Fe_3O_4 NPC catalyzed signal amplification biosensor (C).

3.2. Sandwich Recognition of Van and Aptamer Capture *L. monocytogenes*

To demonstrate that *L. monocytogenes* could be recognized by Van and aptamer simultaneously, confocal microscopy was utilized to observe *L. monocytogenes* stained with the molecular recognition agents tagged with fluorescence probes. Van tagged with RhB (Van-RhB) and aptamer labeled with FITC (aptamer-FITC) were adopted to serve as red and green fluorescence tracers, respectively.

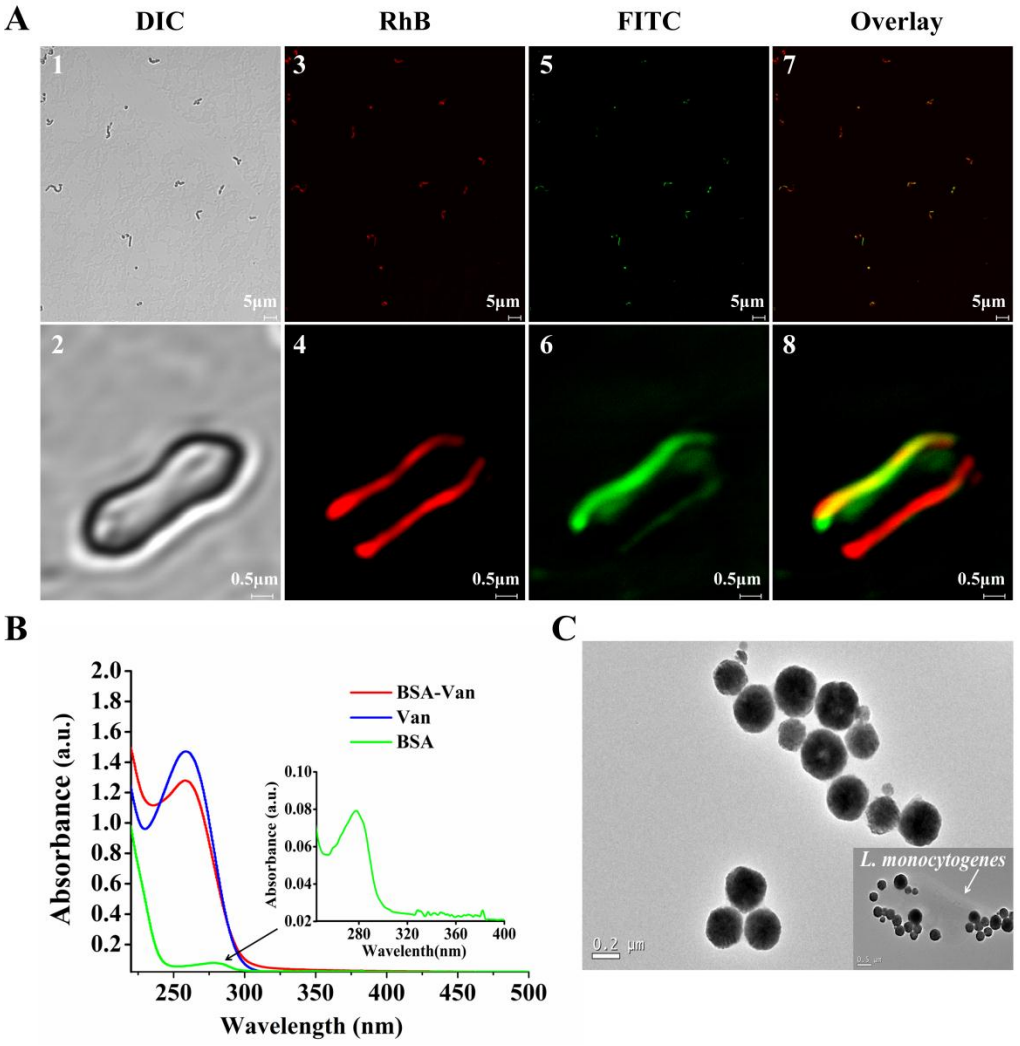

Fig. 2. (A) Fluorescence micrographs of *L. monocytogenes* stained with RhB labeled Van and FITC labeled aptamer. (1-2) bright field image; (3-4) image of red fluorescence channel; (5-6) image of green fluorescence channel; (7-8) image merged from green and red; (B) The UV-Vis absorbance

spectra of BSA-Van, BSA, and the actived Van; (C) TEM images of Fe_3O_4 NP, and Fe_3O_4 NP probe captured *L. monocytogenes.*

Van-RhB and aptamer-FITC were simultaneously incubated with *L. monocytogenes*. The fluorescence stained *L. monocytogenes* complex was observed under confocal microscopy. The bright field images of the stained *L. monocytogenes* have shown in Fig. 2A (1-2). Fig. 2A (3-4) shows red fluorescence and Fig. 2A (5-6) shows the green fluorescence on the bacterial cells, which arose from the tagged RhB and FITC, respectively. From these figures, it can be clearly observed that the fluorescence probe-tagged molecular recognition agents successfully bound to the cell wall of the bacteria. As shown in Fig. 2A (7-8), after the van-RhB and aptamer-FITC incubated with the *L. monocytogenes*, both red fluorescence and green fluorescence were observed on the outer layer of *L. monocytogenes*, which demonstrated that Van and aptamer simultaneously captured *L. monocytogenes*. This phenomenon was very similar to that form occurring in sandwich immunoassay. The above conclusion enabled us to establish a sandwich complex, which could be formed as Nanoprobe/*L. monocytogenes*/BSA-Van.

3.3. Functional Analysis of BSA-Van

Though centrifugation, the purified BSA-Van conjugates were separated from excessive uncombined Van. The BSA-Van was subjected to UV-visible spectrometry. Fig. 2B shows that the absorbance changes of BSA-Van. The characteristic absorption of Van was clearly seen in BSA-Van, demonstrating Van successful immobilization on BSA. For further verify the antibiotic activity of the BSA-Van, a standard bactericidal halo test was utilized. As shown in Fig. S1, the pure BSA didn't have antibacterial activity, but the intact Van and BSA-Van all showed visual inhibition zones, bacteriostatic ring diameter greater than 7 mm, which proved that the conjugated Van still remained antibacterial activity. The antibacterial activity ensured the vancomycin firmly anchoring to the bacteria. Although Van was activated by EDC and conjugated to BSA, it still retained antibiotic activity.

3.4. Performance of the Fe_3O_4 Naoprobe-Based Biosensor

The nanoprobe is a key factor for the performance of this biosensor, The Fe_3O_4 NP with surface carbonyl moieties were synthesized according to the hydrothermal method, Fig. 2C shows the shape and size of the products, the production examined by TEM. Since Fe_3O_4 NP-aptamer was used as the signal probe to recognize *L. monocytogenes*, the TMB colorimetric detection for *L. monocytogenes* was imported. The dose-response relationship for *L. monocytogenes* assay based on TMB colorimetric detection was shown in Fig. 3A, the color intensity increased with the concentration of *L. monocytogenes* and the limit of the detection was around 5.4×10^5 cfu/mL by naked-eyes. The results show that the nanoprobe-based biosensor was feasible to detect *L. monocytogenes*.

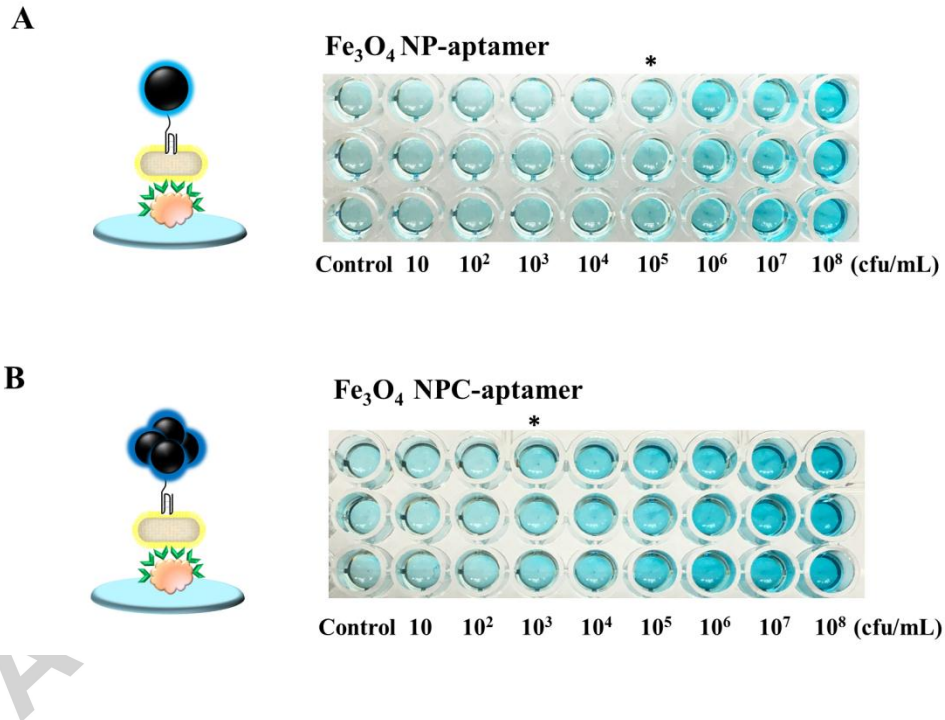

Fig. 3. (A) Absorbance responses for the *L. monocytogenes* assay based on Fe_3O_4 NP-aptamer recognition agent; (B) Absorbance responses for the *L. monocytogenes* assay based on Fe_3O_4 NPC-aptamer recognition agent;

To achieve higher sensitivity, Fe_3O_4 NPC signal amplification probe was used to replace the Fe_3O_4 NP probe. The signal amplification probe composed of two parts: Fe_3O_4 NPC and specific aptamer. As shown in Fig. 3B, under the chosen optimal conditions, *L. monocytogenes* could be

assayed in the concentration range of 5.4×10^3 to 5.4×10^8 cfu/mL, and the detection limit of 5.4×10^3 cfu/mL by naked-eyes. The absorbance response increased with the concentration of *L. monocytogenes* in a linear range of 5.4×10^3 to 5.4×10^8 cfu/mL, as shown in Fig. 4A. The linear regression equation was $y = 0.22054 + 0.10286x$ ($R^2 = 0.99693$), where x and y were stand for the concentration of *L. monocytogenes* and the absorbance response.

In contrast, the detection limit achieved by Fe_3O_4 NP probe-based method is around 5.4×10^5 cfu/mL by naked-eyes, greatly decreased in comparison with that achieved by the Fe_3O_4 NPC probe-based method in visual. The statistical results of the comparison have shown in Fig. 4B. It was noticed that using Fe_3O_4 NPC-aptamer as signal probe was more sensitive than using the Fe_3O_4 NP-aptamer. As described, the nanoparticle cluster catalyzed signal amplification biosensor was conducted by using Van as the capturing agent and NPC-aptamer as the signal tracer. The result further confirmed that using NPC probe replace the individual NP probe as the signal probe could be an efficient way to improve the sensitivity of colorimetric assay.

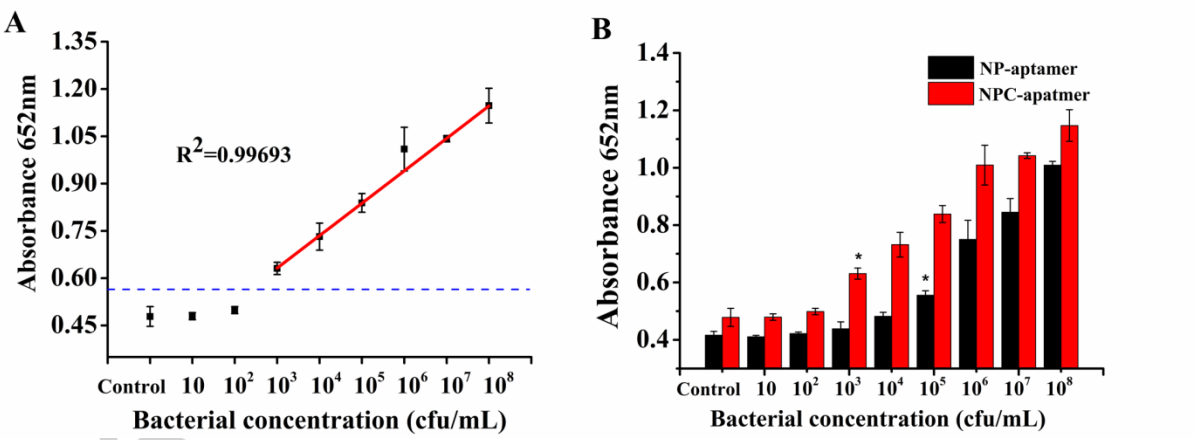

Fig. 4. (A) Absorbance response curves for *L. monocytogenes* assay based on Fe_3O_4 NPC-aptamer; (B) Comparison of the statistical results. All other assay conditions were the chosen optimal conditions.

3.5. Characterization of Fe_3O_4 NPC and Fe_3O_4 NP

Characterization of Fe_3O_4 NPC and Fe_3O_4 NP have shown in Fig. S2A, the hydrodynamic size of Fe_3O_4 NPC increased against with the amounts of PLL increased. The size of Fe_3O_4 NPC reached maximum, when used 12.5 μg of PLL. Further increasing the amounts of PLL, the reaction between

the amino of PLL and the carboxylation of the Fe_3O_4 NP have reached staturation, individual particles couldn't aggregate, the size decreased. Compared to individual Fe_3O_4 NP, NPC could exhibit higher peroxidase catalytic activity, due to the collective effect of Fe_3O_4 NPC. Thus 12.5 μg of PLL was chosen as the optimal condition to cross-linking Fe_3O_4 NP.

Moreover, the change of the zeta potentials was also measured. As shown in Fig. S2B, the zeta potential of NP was negative value, due to the carbonyl moieties of Fe_3O_4 NP. After modified with aptamer, the zeta potential decreased. Compared with NPC-aptamer, the zeta potential of NP-aptamer reduced more significantly, because the most carbonyl moieties of Fe_3O_4 NPC were reacted with the amino of PLL.

3.6. Optimization of Experimental Parameters

As the nanoprobe-based colorimetric method is time-dependent assay, the absorbance intensity changes with the varying concentration of *L. monocytogenes* after adding the 1-Step Ultra-TMB and H_2O_2 (Fig. S5A). The absorbance value reached the highest after incubation 45 min. The whole detection can be completed in 145 min, after a ready-for-use microplate has already been prepared.

The whole detection involved two recognitions, BSA-Van and NPC-aptamer. Thus, the concentration of the two recognitions could be important factors influence the performance of the biosensor. As shown in Fig. S5B, after complete reacted with NPC, 4 mM aptamer showed the highest absorbance value, which indicated that the label of aptamer have been saturated. The concentration of BSA-Van also played an important role in the detection. In this study, BSA-Van firstly coated onto the wells of microplate. It is the key step for the immobilization of target bacteria and the assembly of signal probe. It was found in Fig. S5C that the absorbance value increased obviously when the BSA-Van concentration was fixed above 50 μg/mL. So, 50 μg/mL BSA-Van was chosen to coat the wells. Fig. S5D indicates that the absorbance intensity increased with the increment of amounts of NPC-aptamer. However, when the amounts of NPC-aptamer were above 7.5 μg, the absorbance value increased slowly, indicating that the wells have been saturated with the NPC-aptamer, the absorbance value reach highest at the amounts of 10 μg. All the factors were investigated using *L. monocytogenes* at 5.4×10^8 cfu/mL.

3.7. Specificity of the Signal Amplification Biosensor

The specificity was a key influencing factor for ensuring this strategy feasible. Herein, aptamer was used as the specific molecule recognition to improve the specificity of this nanoprobe-based biosensor. To demonstrate the specificity of the biosensor, *L. monocytogenes*, *E. coli*, *S. aureus*, *Salmonella* and *V. parahaemolyticus* were detected by comparing the absorbance response. Dilution buffer was set as negative control. Fig. 5 shows that the absorbance responses from the *E. coli*, *S. aureus*, *Salmonella* and *V. parahaemolyticus* were similar to the negative signal, but the absorbance response from *L. monocytogenes* was obviously higher than the others. The interference factor (IF) value for these interferents was calculated according to the following equation:

$$\mathbf{IF} = \frac{\mathbf{A} - \mathbf{C}}{\mathbf{B} - \mathbf{C}} \times \mathbf{100}\%$$

where A stands for the absorbance response of the interfering bacteria, B stands for the absorbance response of *L. monocytoge*, C is the responses from the control. The interference factor values of *E. coli*, *Salmonella*, *S. aureus* and *V. parahaemolyticus* were 0.58%, 0.14%, 3.4% and 0.15%, respectively. The results further illustrated that the assay of *L. monocytogenes* was not be interfered by other foodborne pathogens, due to using the NPC-aptamer as specific recognition.

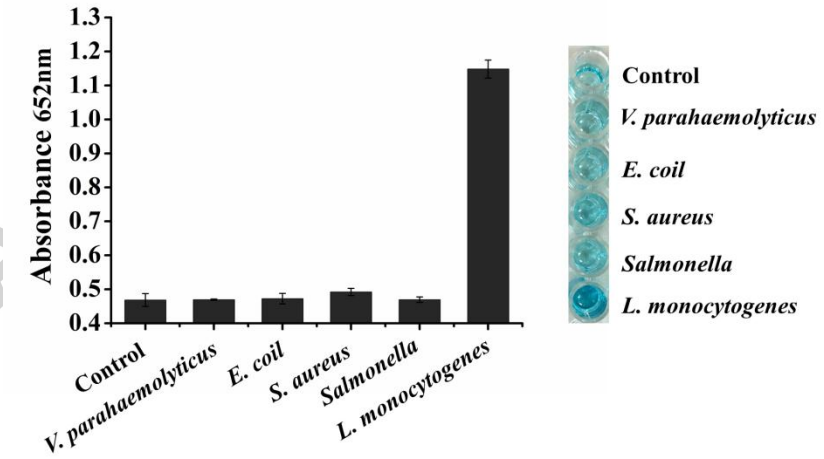

Fig. 5. The absorbance responses to *L. monocytogenes*, *E. coli*, *Salmonella*, *S. aureus* and *V. parahaemolyticus*. The concentrations of all bacteria were 5.4×10^8 cfu/mL. All assay conditions were the chosen optimal conditions.

3.8. Application in Real Sample Assay

Three milk samples were spiked with *L. monocytogenes* standard solutions at different known concentrations and assayed with the proposed method. The relative standard derivations (RSDs) for the detections of *L. monocytogenes* at low concentration (5.4×10^3 cfu/mL), medium concentration (5.4×10^6 cfu/mL) and high concentration (5.4×10^8 cfu/mL) were all below 7.1%, showing acceptable repeatability. Table 1 shows acceptable recoveries ranging from 89.8% to 102.7%, demonstrating the reliability and application potential of the biosensor in real sample assay, which based on the nanoparticle cluster catalyzed signal amplification.

Table 1. Recovery test of *L. monocytogenes* spiked in milk samples using the proposed method

Sample no.	Spiked (cfu/mL)	Found (cfu/mL)	RSD (%)	Recorvery (%)
milk 1	5.4×10^3	5.4×10^3	3.2	101.6
	5.4×10^6	5.5×10^6	2.4	102.7
	5.4×10^8	5.4×10^8	2.2	100.6
milk 2	5.4×10^3	5.5×10^3	4.9	102.3
	5.4×10^6	5.2×10^6	3.0	97.4
	5.4×10^8	5.4×10^8	7.1	101.7
milk 3	5.4×10^3	5.3×10^3	2.1	98.2
	5.4×10^6	4.8×10^6	3.9	89.2
	5.4×10^8	4.9×10^8	2.5	90.8

4. Conclusion

In conclusion, the Fe_3O_4 NPC catalyzed signal amplification biosensor was proposed to visual detect the whole cells of foodborne pathogenic based on the NPC-aptamer. This strategy was demonstrated by absorbance response and color change of the substrate, which catalyzed by the NPC.

This approach showed satisfied sensitivity and wide linear range, *L. monocytogenes* whole cells could be directly assayed within a linear range of 5.4×10^3-10^8 cfu/mL and a visual limit of detection of 5.4×10^3 cfu/mL. The Fe_3O_4 NPC signal amplification probe insured that the strategy was feasible for the sensitive and visual detect foodborne pathogenic, and the cross-linking interaction model of Fe_3O_4 NPC will play a guiding role for the design of nanoparticle catalyzed signal amplification biosensor. As a convenient approach, it did not demand such pretreatments as bacteria culture and nucleic acid extracting, thus allowing rapid and simple assay of pathogens. This strategy has a potential be extended to point-of-care and in-field analyses of other foodborne pathogens.

Acknowledgments

This work was supported by the National Natural Science Foundation of China [21475048], the National Science Fund for Distinguished Young Scholars of Guangdong Province [2014A030306008], the Project of Guangzhou Science and Technology Plan [201508020003], and the Program of the Pearl River Young Talents of Science and Technology in Guangzhou [2013J2200021], the Special Support Program of Guangdong Province (2014TQ01R599), and the Outstanding Young Teacher Training Program of Guangdong Province (HS2015004)

References

Asiello, P.J., Baeumner, A.J., 2011. Miniaturized isothermal nucleic acid amplification, a review. Lab Chip 11(8), 1420-1430.

Azmi, S., Jiang, K., Stiles, M., Thundat, T., Kaur, K., 2015. Detection of *Listeria monocytogenes* with short peptide fragments from class IIa bacteriocins as recognition elements. ACS Comb Sci 17(3), 156-163.

Chua, A., Yean, C.Y., Ravichandran, M., Lim, B., Lalitha, P., 2011. A rapid DNA biosensor for the molecular diagnosis of infectious disease. Biosensors and Bioelectronics 26(9), 3825-3831.

Compton, J., 1991. Nucleic acid sequence-based amplification. Nature 350(6313), 91-92.

De Vocht, C., Ranquin, A., Van Ginderachter, J., Vanhaecke, T., Rogiers, V., Van Gelder, P., Versées, W., Steyaert, J., 2010. Polymeric nanoreactors for enzyme replacement therapy of MNGIE. Journal of Controlled Release 148(1), e19-e20.

Ding, J., Lei, J., Ma, X., Gong, J., Qin, W., 2014. Potentiometric aptasensing of *Listeria monocytogenes* using protamine as an indicator. Anal Chem 86(19), 9412-9416.

Doumith, M., Buchrieser, C., Glaser, P., Jacquet, C., Martin, P., 2004. Differentiation of the major *Listeria monocytogenes* serovars by multiplex PCR. J Clin Microbiol 42(8), 3819-3822.

Duan, D., Fan, K., Zhang, D., Tan, S., Liang, M., Liu, Y., Zhang, J., Zhang, P., Liu, W., Qiu, X., Kobinger, G.P., Gao, G.F., Yan, X., 2015. Nanozyme-strip for rapid local diagnosis of Ebola. Biosens Bioelectron 74, 134-141.

Edwards, K., Johnstone, C., Thompson, C., 1991. A simple and rapid method for the preparation of plant genomic DNA for PCR analysis. Nucleic Acids Res 19(6), 1349.

Fan, K., Cao, C., Pan, Y., Lu, D., Yang, D., Feng, J., Song, L., Liang, M., Yan, X., 2012. Magnetoferritin nanoparticles for targeting and visualizing tumour tissues. Nat Nanotechnol 7(7), 459-464.

Gao, H., Yang, S., Han, J., Xiong, J., Kong, W., Li, C., Liao, G., Fu, Z., 2015. Double-site recognition of pathogenic bacterial whole cells based on an antibiotic-affinity strategy. Chem Commun (Camb) 51(62), 12497-12500.

Gao, L., Zhuang, J., Nie, L., Zhang, J., Zhang, Y., Gu, N., Wang, T., Feng, J., Yang, D., Perrett, S., Yan, X., 2007. Intrinsic peroxidase-like activity of ferromagnetic nanoparticles. Nat Nanotechnol 2(9), 577-583.

Gao, Z., Hou, L., Xu, M., Tang, D., 2014. Enhanced colorimetric immunoassay accompanying with enzyme cascade amplification strategy for ultrasensitive detection of low-abundance protein. Sci Rep 4, 3966.

Jiang, T., Song, Y., Wei, T., Li, H., Du, D., Zhu, M.-J., Lin, Y., 2016. Sensitive detection of *Escherichia coli O157: H7* using Pt–Au bimetal nanoparticles with peroxidase-like amplification. Biosensors and Bioelectronics 77, 687-694.

Kell, A.J., Stewart, G., Ryan, S., Peytavi, R., Boissinot, M., Huletsky, A., Bergeron, M.G., Simard, B., 2008. Vancomycin-modified nanoparticles for efficient targeting and preconcentration of Gram-positive and Gram-negative bacteria. ACS Nano 2(9), 1777-1788.

Knopp, D., Tang, D., Niessner, R., 2009. Review: bioanalytical applications of biomolecule-functionalized nanometer-sized doped silica particles. Anal Chim Acta 647(1), 14-30.

Kong, W., Xiong, J., Yue, H., Fu, Z., 2015. Sandwich fluorimetric method for specific detection of *Staphylococcus aureus* based on antibiotic-affinity strategy. Anal Chem 87(19), 9864-9868.

Law, J.W., Ab Mutalib, N.S., Chan, K.G., Lee, L.H., 2014. Rapid methods for the detection of foodborne bacterial pathogens: principles, applications, advantages and limitations. Front Microbiol 5, 770.

Lazcka, O., Del Campo, F.J., Munoz, F.X., 2007. Pathogen detection: a perspective of traditional methods and biosensors. Biosensors and bioelectronics 22(7), 1205-1217.

Lee, S.-H., Ahn, J.-Y., Lee, K.-A., Um, H.-J., Sekhon, S.S., Park, T.S., Min, J., Kim, Y.-H., 2015. Analytical bioconjugates, aptamers, enable specific quantitative detection of Listeria monocytogenes. Biosensors and Bioelectronics 68, 272-280.

Lee, S., Rakic-Martinez, M., Graves, L.M., Ward, T.J., Siletzky, R.M., Kathariou, S., 2013. Genetic determinants for cadmium and arsenic resistance among *Listeria monocytogenes* serotype 4b isolates from sporadic human listeriosis patients. Appl Environ Microbiol 79(7), 2471-2476.

Lemaitre, M., Bayard, B., Lebleu, B., 1987. Specific antiviral activity of a poly (L-lysine)-conjugated oligodeoxyribonucleotide sequence complementary to vesicular stomatitis virus N protein mRNA initiation site. Proceedings of the National Academy of Sciences 84(3), 648-652.

Leone, G., van Gemen, B., Schoen, C.D., van Schijndel, H., Kramer, F.R., 1998. Molecular beacon probes combined with amplification by NASBA enable homogeneous, real-time detection of RNA. Nucleic Acids Res 26(9), 2150-2155.

Liang, M., Fan, K., Pan, Y., Jiang, H., Wang, F., Yang, D., Lu, D., Feng, J., Zhao, J., Yang, L., Yan, X., 2013. Fe_3O_4 magnetic nanoparticle peroxidase mimetic-based colorimetric assay for the rapid detection of organophosphorus pesticide and nerve agent. Anal Chem 85(1), 308-312.

Liu, C., Jia, Q., Yang, C., Qiao, R., Jing, L., Wang, L., Xu, C., Gao, M., 2011. Lateral flow immunochromatographic assay for sensitive pesticide detection by using Fe_3O_4 nanoparticle aggregates as color reagents. Anal Chem 83(17), 6778-6784.

McGregor, L.M., Gorin, D.J., Dumelin, C.E., Liu, D.R., 2010. Interaction-Dependent PCR: Identification of Ligand− Target Pairs from Libraries of Ligands and Libraries of Targets in a Single Solution-Phase Experiment. J Am Chem Soc 132(44), 15522-15524.

Notomi, T., Okayama, H., Masubuchi, H., Yonekawa, T., Watanabe, K., Amino, N., Hase, T., 2000. Loop-mediated isothermal amplification of DNA. Nucleic Acids Res 28(12), e63-e63.

Parida, M., Sannarangaiah, S., Dash, P.K., Rao, P., Morita, K., 2008. Loop mediated isothermal amplification (LAMP): a new generation of innovative gene amplification technique; perspectives in clinical diagnosis of infectious diseases. Rev Med Virol 18(6), 407-421.

Qu, Z., Xu, H., Xu, P., Chen, K., Mu, R., Fu, J., Gu, H., 2014. Ultrasensitive ELISA using enzyme-loaded nanospherical brushes as labels. Anal Chem 86(19), 9367-9371.

Shan, S., Lai, W., Xiong, Y., Wei, H., Xu, H., 2015. Novel strategies to enhance lateral flow immunoassay sensitivity for detecting foodborne pathogens. J Agric Food Chem 63(3), 745-753.

Tekin, H.C., Gijs, M.A., 2013. Ultrasensitive protein detection: a case for microfluidic magnetic bead-based assays. Lab Chip 13(24), 4711-4739.

Tomita, N., Mori, Y., Kanda, H., Notomi, T., 2008. Loop-mediated isothermal amplification (LAMP) of gene sequences and simple visual detection of products. Nat Protoc 3(5), 877-882.

Vaisocherová-Lísalová, H., Víšová, I., Ermini, M.L., Špringer, T., Song, X.C., Mrázek, J., Lamačová, J., Lynn, N.S., Šedivák, P., Homola, J., 2016. Low-fouling surface plasmon resonance biosensor for multi-step detection of foodborne bacterial pathogens in complex food samples. Biosensors and Bioelectronics.

Valderrama, W.B., Dudley, E.G., Doores, S., Cutter, C.N., 2015. Commercially available rapid methods for detection of selected foodborne pathogens. Crit Rev Food Sci Nutr(just-accepted), 00-00.

Van Ness, J., Van Ness, L.K., Galas, D.J., 2003. Isothermal reactions for the amplification of oligonucleotides. Proceedings of the National Academy of Sciences 100(8), 4504-4509.

Wei, H., Wang, E., 2013. Nanomaterials with enzyme-like characteristics (nanozymes): next-generation artificial enzymes. Chem Soc Rev 42(14), 6060-6093.

Yang, S., Ouyang, H., Su, X., Gao, H., Kong, W., Wang, M., Shu, Q., Fu, Z., 2016. Dual-recognition detection of *Staphylococcus aureus* using vancomycin-functionalized magnetic beads as concentration carriers. Biosens Bioelectron 78, 174-180.

Zhang, H., Zhang, Y., Lin, Y., Liang, T., Chen, Z., Li, J., Yue, Z., Lv, J., Jiang, Q., Yi, C., 2015. Ultrasensitive detection and rapid identification of multiple foodborne pathogens with the naked eyes. Biosensors and Bioelectronics 71, 186-193.

Zhu, L., He, J., Cao, X., Huang, K., Luo, Y., Xu, W., 2016. Development of a double-antibody sandwich ELISA for rapid detection of *Bacillus Cereus* in food. Sci Rep 6.

Zhu, M., Liu, W., Liu, H., Liao, Y., Wei, J., Zhou, X., Xing, D., 2015. Construction of Fe_3O_4/Vancomycin/PEG Magnetic Nanocarrier for Highly Efficient Pathogen Enrichment and Gene Sensing. ACS Appl Mater Interfaces 7(23), 12873-12881.

Zhuang, J., Fan, K., Gao, L., Lu, D., Feng, J., Yang, D., Gu, N., Zhang, Y., Liang, M., Yan, X., 2012. Ex vivo detection of iron oxide magnetic nanoparticles in mice using their intrinsic peroxidase-mimicking activity. Mol Pharm 9(7), 1983-1989.

Highlights

- Nanoparticle cluster catalyzed signal amplification biosensor.
- Fe_3O_4 nanoparticle cluster possesses high efficient peroxidase-like activity.
- A detection limit of 5.4×10^3 cfu/mL *L. Monocytogenes* was obtained.
- The developed biosensor can be used for visual detection of foodborne pathogens.